Am J Clin Exp Urol 2022;10(6):377-389
www.ajceu.us /ISSN:2330-1910/AJCEU0148577

Original Article

Stem cells from a malignant rat prostate cell line generate prostate cancers *in vivo*: a model for prostate cancer stem cell propagated tumor growth

Wen-Yang Hu[1], Li-Feng Liu[1], Parivash Afradiasbagharani[1], Ran-Li Lu[1], Zhen-Long Chen[2], Dan-Ping Hu[1], Lynn A Birch[1], Gail S Prins[1]

[1]*Department of Urology, University of Illinois at Chicago, Chicago, IL 60612, USA;* [2]*Division of Endocrinology, Diabetes and Metabolism, Beth Israel Deaconess Medical Center, Boston, MA 02215, USA*

Received December 16, 2022; Accepted December 25, 2022; Epub December 25, 2022; Published December 30, 2022

Abstract: Cancer stem cells (CSCs) are resistant to conventional cancer therapies, permitting the repopulation of new tumor growth and driving disease progression. Models for testing prostate CSC-propagated tumor growth are presently limited yet necessary for therapeutic advancement. Utilizing the congenic nontumorigenic NRP152 and tumorigenic NRP154 rat prostate epithelial cell lines, the present study investigated the self-renewal, differentiation, and regenerative abilities of prostate stem/progenitor cells and developed a CSC-based PCa model. NRP154 cells expressed reduced levels of tumor suppressor caveolin-1 and increased p-Src as compared to NRP152 cells. Gene knockdown of caveolin-1 in NRP152 cells upregulated p-Src, implicating their role as potential oncogenic mediators in NRP154 cells. A FACS-based Hoechst exclusion assay revealed a side population of stem-like cells (0.1%) in both NRP152 and NRP154 cell lines. Using a 3D Matrigel culture system, stem cells from both cell lines established prostaspheres at a 0.1% efficiency through asymmetric self-renewal and rapid proliferation of daughter progenitor cells. Spheres derived from both cell lines contained $CD117^+$ and $CD133^+$ stem cell subpopulations and basal progenitor cell subpopulations ($p63^+$ and $CK5^+$) but were negative for luminal cell CK8 markers at day 7. While some NRP152 sphere cells were androgen receptor (AR) positive at this timepoint, NRP154 cells were AR^- up to 30 days of 3D culture. The regenerative capacity of the stem/progenitor cells was demonstrated by *in vivo* tissue recombination with urogenital sinus mesenchyme (UGM) and renal grafting in nude mice. While stem/progenitor cells from NRP152 spheroids generated normal prostate structures, CSCs and progeny cells from NRP154 tumoroids generated tumor tissues that were characterized by immunohistochemistry. Atypical hyperplasia and prostatic intraepithelial neoplasia (PIN) lesions progressed to adenocarcinoma with kidney invasion over 4 months. This provides clear evidence that prostate CSCs can repopulate new tumor growth outside the prostate gland that rapidly progresses to poorly differentiated adenocarcinoma with invasive capabilities. The dual *in vitro/in vivo* CSC model system presented herein provides a novel platform for screening therapeutic agents that target prostate CSCs for effective combined treatment protocols for local and advanced disease stages.

Keywords: Prostate cancer, cancer stem cells, prostasphere

Introduction

Prostate cancer (PCa) is the leading cause of cancer deaths in men in the Western world with estimates of 34,500 PCa deaths in the U.S. for 2022 [1]. Sixty-five percent of PCa patients will develop metastatic cancer and eventually progress to the castration-resistant stage where limited treatment options remain a major challenge for clinicians. The cancer stem cell theory [2] posits that PCa progression, metastasis, and tumor repopulation after therapeutic intervention are, in part, due to survival, self-renewal, and propagation of prostate cancer stem cells (CSC) within tumors which are resistant to conventional PCa therapies. While the bulk of tumors is constituted by non-stem cancer cells that can be highly proliferative, most have limited capacity to form secondary tumors. In contrast, highly tumorigenic CSCs are rare immortal cells that can self-renew through asymmetric division, give rise to many cell types that recon-

stitute the tumor [3]. As such, CSCs are considered an Achilles' heel in PCa that leads to therapeutic resistance.

CSCs may originate from oncogenic transformation of stem cells, progenitor cells, or differentiated cancer cells that through oncogenic plasticity, acquire key stem-like cell characteristics. While this rare cell population is undoubtedly heterogeneous across and perhaps within tumors, CSCs in most tumors, including PCa, express common genes and cell surface proteins associated with normal stem cells.

A major therapeutic challenge for PCa therapy is the need for small molecules and chemotherapy agents that target CSCs and can be used in combination with conventional therapies for effective tumor control. To meet that need, both *in vitro* and *in vivo* models for studying benign and tumorigenic prostate stem cells are required for the testing and evaluation of promising agents. Immortalized cell lines have proven critical for cancer research, as patient material is limited. Of note, many cancer cell lines, including PCa lines, contain a minor population of stem-like cells [4-6] that can be used for discovery of therapeutic targets. The challenge remains to interpret and compare such results directly with benign prostate stem cells and stem-like cancer cells *in vivo*.

In the present study, we developed *in vivo* models for benign and cancerous prostate growth using stem/progenitor cells isolated from the nontumorigenic NRP152 and tumorigenic NRP-154 rat prostate epithelial cell lines. NRP152 and NRP154 are two stable cell lines clonally derived from the dorsal-lateral prostate lobes of two Lobund/Wistar rats treated with carcinogen *N*-methyl-*N*-nitrosourea (MNU) and testosterone propionate (TP) [7]. While NRP152 cells are nontumorigenic in subcutaneous and renal grafts [7, 8], they are considered premalignant due to an aneuploid karyotype. In culture, NRP152 cells express androgen receptors (ARs), are responsive to multiple hormones, and due to expressions of cytokeratin 14 but not cytokeratins 8/18, are considered basal in origin. These androgen-responsive cells exhibit basal epithelial cell characteristics when cultured under normal growth conditions (high serum) and differentiate to a luminal epithelial phenotype under growth-restrictive conditions (low serum), with the addition of TGFβ1 or overexpression of Hoxb13 [9, 10]. NRP154 cells are also aneuploid, however, when grafted subcutaneously, they consistently form tumors in athymic mice. NRP154 cells lack detectable AR but express cytokeratins 8/18 and are considered of luminal origin [7]. Herein, a minor population of resident stem-like cells was documented in both cell lines and upon transfer of 2D cultures to 3D Matrigel cultures, the NRP152 and NRP154 stem-like cells established benign and cancerous prostaspheres, respectively, comprised mostly of rapidly proliferating daughter progenitor cells. Using prostasphere cell-urogenital mesenchyme (UGM) recombinants grafted under the kidney capsule in nude mice, an organized prostate ductal structure was established from the NRP152 progenitor cells. Of particular significance, the cancer stem/progenitor cells from NRP154 spheroids mixed with UGM generated prostate cancerous structures in the renal grafts that progressed to kidney invasion over time. These findings support the existence of cancer stem-like cells that reseed and propagate new tumor growth. Further, the model systems are useful for future studies of PCa originating from transformed stem/progenitor cells and will enable the screening and selection of the chemotherapeutic agents that target the elusive prostate CSC population.

Material and methods

Animals

All animals were handled according to the principles and procedures of the Guiding Principles for the Care and Use of Animal Research and the experiments were approved by the Institutional Animal Care Committee. Timed pregnant female Sprague Dawley rats were purchased from Harlan (Indianapolis, IN). Male nude mice (6-week old) were purchased from Charles River (Wilmington, MA) and housed individually in a temperature (21°C) and light (14 h light/10 h dark) controlled room with standard Purina chow (Ralston-Purina, St. Louis, MO) *ad libitum*.

Prostate epithelial cells culture

Nontumorigenic NRP152 cells and tumorigenic NRP154 cells were generously provided by Prof. David Danielpour (Case Western University, Cleveland, OH). The NRP152 cells used in

this study were between passages 20 and 25 and the NRP154 cells were between passages 15 to 20. Cells were grown in a 5% CO_2 atmosphere at 37°C under normal growth conditions in GM2 (DMEM/F12 containing 5% fetal bovine serum, 5 μg/ml bovine insulin, 20 ng/ml EGF, 10 ng/ml cholera toxin and 0.1 μM dexamethasone) as described [7, 9]. Cultures were maintained at less than 70% confluence. Cells were passaged at ~70% confluence with 0.05% trypsin/EDTA every 5-7 days. Viable cell numbers were determined by hematocytometry with trypan blue exclusion.

Western blot

Gene knockdown of caveolin-1 in NRP152 cells was achieved by incubating cells with 120 nM siCav-1 solution overnight. Cells were harvested after 3 days. NRP152 and NRP154 cells from 2D cultures were lysed by sonication for 10 min at 4°C in 2% ODG (Tris buffer pH 7.5, 50 mM Tris, 150 mM NaCl, 1 mM NaF, 1 mM EDTA, 1 mM Na_3VO_4, 44 μg/ml phenylmethylsulfonyl fluoride [PMSF], 1% protease inhibitor cocktail). The lysates were centrifuged for 20 min at 16,000 × *g* at 4°C. The proteins were eluted from the supernatant with Laemmle buffer, 20 μg protein was separated via 10% SDS-PAGE gels, transferred to nitrocellulose membranes, followed by immunoblotting with primary and secondary antibodies as described previously [11]. Primary antibodies used were rabbit anti-Cav-1 (BD Biosciences, San Diego, CA), mouse anti-p-Cav-1 (BD Biosciences), mouse anti-actin (BD Biosciences), and rabbit anti-Src and p-Src (Tyr418) (Cell Signaling, Danvers, MA). Horseradish peroxidase (HRP) conjugated secondary antibodies (Invitrogen, Molecular Probes Inc., Eugene, OR) were used. Membrane-bound antibodies were visualized using the SuperSignal™ West Femto Kit (ThermoFisher Scientific, Waltham, MA).

Hoechst exclusion side-population assay

NRP152 and NRP154 cells from 2D cultures were split into two vials and pre-incubated for 10 min with or without 50 μM verapamil hydrochloride (Sigma-Aldrich Inc., St. Louis, MO) which inhibits ABCG2 transporter protein expressed at high levels in stem cells, blocking their Hoechst exclusion ability. Cells were next incubated in 0.5 μg/ml Hoechst 33342 (Sigma-Aldrich) in Hanks' balanced salt solution, 10% FBS, 1% D-glucose, 20 mM HEPES for 30 min at 37°C, washed in PBS and incubated with 1 μg/ml Propidium iodide (PI) labeling for dead cell exclusion. Hoechst-stained cells were analyzed by single-channel FACS (CyAn™ ADP Analyzer) to gate a small side-population as prostate stem-like cells. The fraction of stem-like cells was calculated by the % difference in Hoechst excluding cells incubated with and without verapamil. Unstained cells were used to determine the window gating for side populations [12].

Prostasphere assay

Prostasphere culture conditions were modifications of previously published protocols [12-15]. Briefly, 1 × 10^5 NRP152 or NRP154 cells were resuspended in 1:1 Matrigel (BD Biosciences)/PrEGM (Lonza, Walkersville, MD) in a total volume of 200 μl. Cells in suspension were plated in 12-well plates and the semi-gel was allowed to solidify at 37°C for 15 min prior to adding 1 ml of PrEGM. The medium was replenished every 3 days. Prostasphere formation and growth were monitored by microscopy and real-time imaging using a Zeiss Axiovert 200 inverted microscope with an automated X-Y-Z stage and Axiocam HRm digital camera (Carl Zeiss MicroImaging, Inc., Thornwood, NY).

For *in vitro* characterization, prostaspheres at days 7, 10, and 30 were harvested for ICC histology studies. For ICC, day 7 spheres were transferred to an 8-well chamber slide and cultured overnight to permit cell attachment. Cells were fixed in 1:1 methanol: acetone solution and processed for immunocytochemistry staining. For *in vitro* differentiation analysis, prostaspheres cultured for 10 to 30 days were removed from Matrigel by dispase, fixed, and embedded in paraffin for sectioning followed by H&E and IHC staining [13].

For tissue recombination and *in vivo* growth, the Matrigel with day 7 prostasphere cultures were digested by incubation in 500 μl of dispase solution (1 mg/ml; Invitrogen, Carlsbad, CA) for 30 min at 37°C. Digested cultures were pelleted, resuspended in 1 ml type I collagenase solution (190 units/ml; Invitrogen), and incubated for 45 min at 37°C. Dissociated cells were pelleted, resuspended, and incubated in 0.05% trypsin/EDTA (Invitrogen) for 10 min at room temperature, passed 5-10 times through

a 27-gauge syringe, and lastly through a 40 μm filter. The dissociated single cells were counted by hemocytometer prior to their use for renal grafts [13, 14].

Immunocytochemistry and immunohistochemistry

Immunocytochemistry (ICC) staining was performed on prostasphere cells grown overnight in chamber slides to permit limited outgrowth of the cells and optimal immunofluorescent labeling. Briefly, day 7 prostaspheres were transferred to collagen-coated 8-well chamber slides and cultured in PrEGM for 16 hr at 37°C for attachment. The spheres were washed 3 times in PBS and fixed with ice-cold acetone/methanol (1:1) solution at -20°C for 15 minutes. Prostaspheres were washed with PBS followed by blocking, primary and secondary antibodies incubation, mounting, and imaging as described [13, 14]. Primary antibodies used with prostaspheres were rabbit anti-CD133 (Abcam, Cambridge, MA), rabbit anti-CD117 (c-Kit), rabbit anti-p63, rabbit anti-β-catenin (Santa Cruz Biotechnology, Santa Cruz, CA), rabbit anti-CK5, rabbit anti-CK8 (Epitomics, Burlingame, CA), and rabbit anti-AR, PG21 [16].

Immunohistochemistry (IHC) was performed on paraffin-embedded sections of renal graft tissues for the identification of tissue type, pathology, and differentiation status of the grafts as previously described [13, 14]. Tissue paraffin sections were deparaffinized and heat-treated for 3 min in antigen retrieval solution Tris-EDTA Buffer (10 mM Tris Base, 1 mM EDTA Solution, 0.05% Tween 20, pH 9.0) using a Decloaker pressure cooker (Biocare Medical, Walnut Creek, CA). Sections were blocked with 5% NGS-PBST (5% normal goat serum in 0.01 M PBS with 0.25% Triton-X-100) for 45 min followed by incubation with primary antibody diluted in 2% NGS-PBST at 4°C overnight. Primary antibodies used include rabbit anti-p63 (Santa Cruz), rabbit anti-Ki-67 (Abcam, Waltham, MA), guinea pig anti-CK8/18 (American Research Products, Belmont, MA), and rabbit anti-CK5, and anti-CK14 (Epitomics). For negative controls, normal goat, rabbit, guinea pig, or mouse IgG was substituted for the primary antibody. The sections were washed with PBS followed by incubation at room temperature for 2 hours with AlexaFluor-488 dye-conjugated goat anti-rabbit, Alexa-Fluor-568 dye-conjugated goat anti-guinea pig secondary antibodies (Invitrogen, Molecular Probes Inc., Eugene, OR) used at 1:500 dilution with PBST containing 2% NGS. Following PBS wash, tissue sections were mounted using VECTASHIELD mounting medium with DAPI (Vector Laboratories, Inc. Burlingame, CA) and photographs were taken with a Zeiss Axiocam microscope imaging system [13, 14].

Tissue recombination and renal grafting

Embryonic day 18 fetuses from timed-pregnant SD rats were collected by Caesarian section, the bladder and urogenital tracts removed, and the urogenital sinus (UGS) dissected free from other structures. The UGS was washed with Hank's-CMF (calcium magnesium free) balanced salt solution and digested with pre-chilled fresh-made 1% trypsin/Hank's digestion solution for 90 min at 4°C (Difco trypsin250, Dickinson and Co., Sparks, MD). After trypsinization, the tissues were transferred by glass pipette to Hank's solution and the trypsin digestion was stopped by the addition of an equal volume of fresh 20% fetal calf serum in Hank's medium for 5 min. The tissues were washed in Hank's-CMF, placed into Hank's-CMF containing 1 mg/ml DNase (Sigma), and using fine forceps, the UGM pad was gently separated from the urogenital epithelium (UGE) under the microscope. After microscopically confirming the absence of UGE, the UGM pads were used for tissue recombination with isolated prostasphere cells.

Day 7 NRP152 and NRP154 prostaspheres grown in 3D cultures were used for tissue recombination and *in vivo* renal grafting. For each graft, ~3000 dispersed prostasphere single cells (above) were mixed with rat UGM from one embryo and re-suspended in 10 μl of growth factor-reduced Matrigel (BD Biosciences). Cell-tissue recombinants were plated on the surface of a 1% agar gel plate (35 × 10 mm petri dish) and incubated at 37°C for 15 min to solidify before adding 200 μl PrEGM followed by incubation in 5% CO_2 at 37°C overnight. The prostate stem/progenitor cell/UGM recombinants were grafted under the renal capsule of male nude mice using aseptic techniques as previously described [13, 14]. To ensure adequate androgenic support for prostate growth

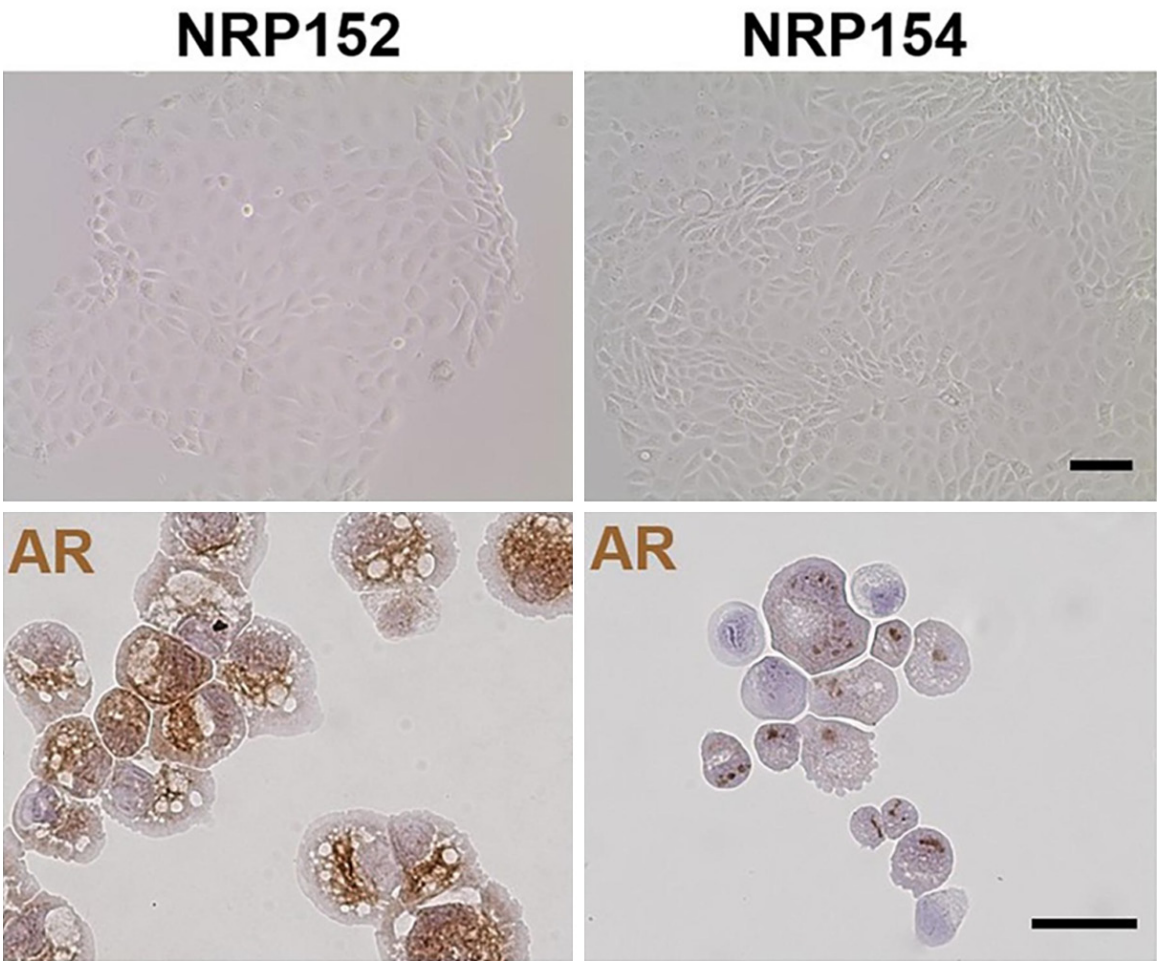

Figure 1. Established 2D cultures of rat prostate NRP152 and NRP154 cell lines. ICC staining documents the presence of AR protein in non-tumorigenic NRP152 cells and the absence of AR protein in the malignant NRP154 cells. Bar = 50 μm.

in the hypogonadal nude mice, the mice were supplemented with Silastic testosterone capsules (1.02 mm inner diameter, 2.16 mm outer diameter; Dow Corning, Midland, MI) containing 3.5 mg crystalline testosterone (Sigma-Aldrich, St. Louis, MO) at the time of grafting. Grafts with UGM or UGE alone were used for quality controls [13, 14].

Results

NRP152 and NRP154 cells in 2D culture

Non-tumorigenic NRP152 and tumorigenic NRP154 cells were established in 2D culture and examined for differential expression of key signaling molecules involved in tumorigenesis. It was previously shown by Northern blots and AR binding assays that NRP152 cells express AR while NRP154 cells lack AR expression, and this was confirmed at the protein level by ICC (**Figure 1**). To identify additional mediators of the differential tumorigenic capacities of these two cell types, we screened for the activational status of multiple signaling regulators by Western blot. While levels of PTEN, total and phospho-Akt (S473), e-cadherin and β-catenin were not different between the two cell lines (data not shown), there was marked suppression of total caveolin-1, p-Cav-1 (Tyr14), and strong activation of p-Src (Tyr418) in NRP154 cells compared to NRP152 cells (**Figure 2A**). This is significant since caveolin-1 can act as a tumor suppressor in a stage-dependent manner [17] and constitutively active Src has a high potential to transform the prostate epithelium [18, 19]. As these intra-membrane signaling regulators are known to interact with each other, we used siRNA to knock down total caveolin-1 in NRP152 cells. This led to a marked

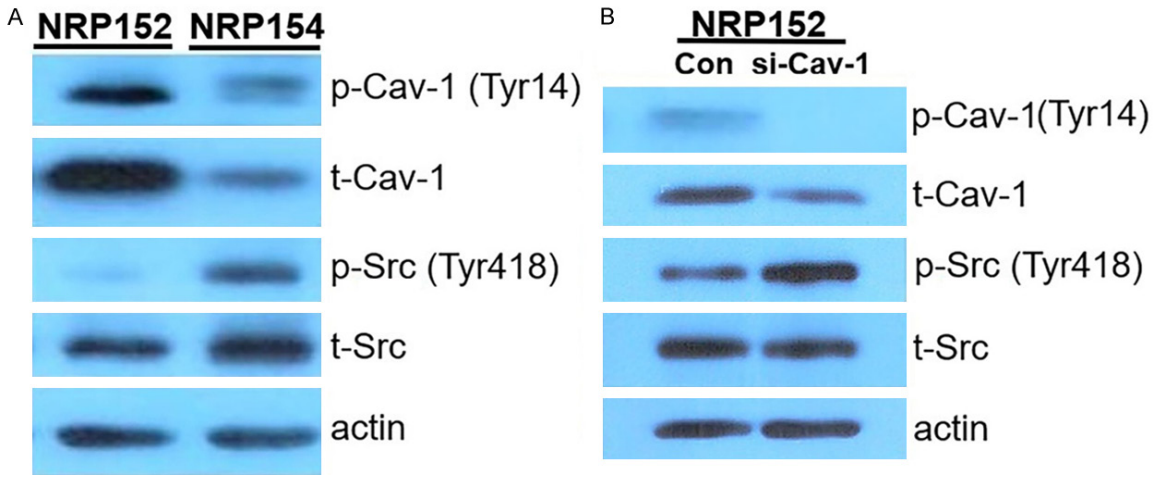

Figure 2. Western blot analysis of caveolin-1 and Src in NRP152 and NRP154 cell lines. A. Total and phosphorylated (Tyr14) Caveolin-1 was markedly lower in NRP154 cells compared to NRP152 cells while phosphorylated Src (Tyr418) levels were elevated in NRP154 cells. B. Caveolin-1 knockdown by siRNA in NRP152 cells resulted in increased phosphorylation of Src, resembling a profile seen in NRP154 cells.

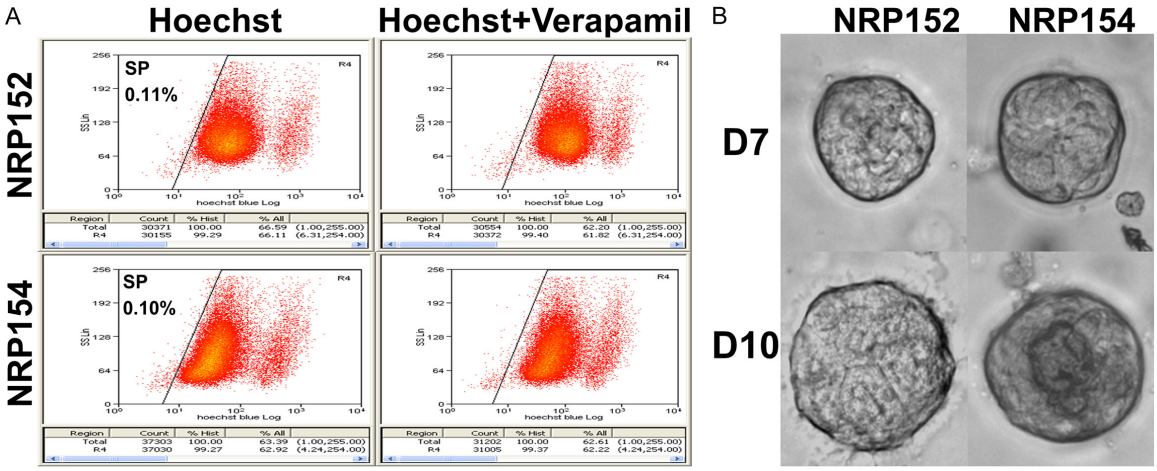

Figure 3. Identification of stem cells in NRP152 and NRP154 cells. A. Flow cytometry analysis using Hoechst exclusion assay reveals a side population (~0.1%) of stem-like cells in both NRP152 and NRP154 cell lines. B. In 3D Matrigel culture, a small number of stem-like cells from both NRP152 and NRP154 cell lines generate prostaspheres through asymmetric self-renewal to generate daughter progenitor cells that rapidly proliferate to form growing spheroids of lineage committing progenitors at day 7 and day 10. Bar = 50 μm.

increase in p-Src (Tyr418) levels (**Figure 2B**), the active form of Src, which suggests that suppression of caveolin-1 drives constitutive activation of p-Src a possible key component of the tumorigenic activity in NRP154 cells.

Presence of stem cells within NRP152 and NRP154 cells

A minor population of stem cells has been shown to exist in many benign and cancerous cell lines, including PCa cell lines [4-6]. To identify stem-like cell populations in the two NRP cell lines, Hoechst-exclusion side population assays were performed. Stem cells express high levels of ABCG2 transporter which effluxes Hoechst33342 dye, whereas lineage-committed cells and differentiated cells have limited ABCG2 expression and thus retain the Hoechst dye. When separated by FACS, the low Hoechst retaining cells are separated from the bulk of the differentiated cells (**Figure 3A**). A parallel cell sample treated with verapamil, an ABCG2 inhibitor, results in Hoechst retention in the stem cell population as well. This can be quantitated as the difference between cell numbers in the separate fractions without and with vera-

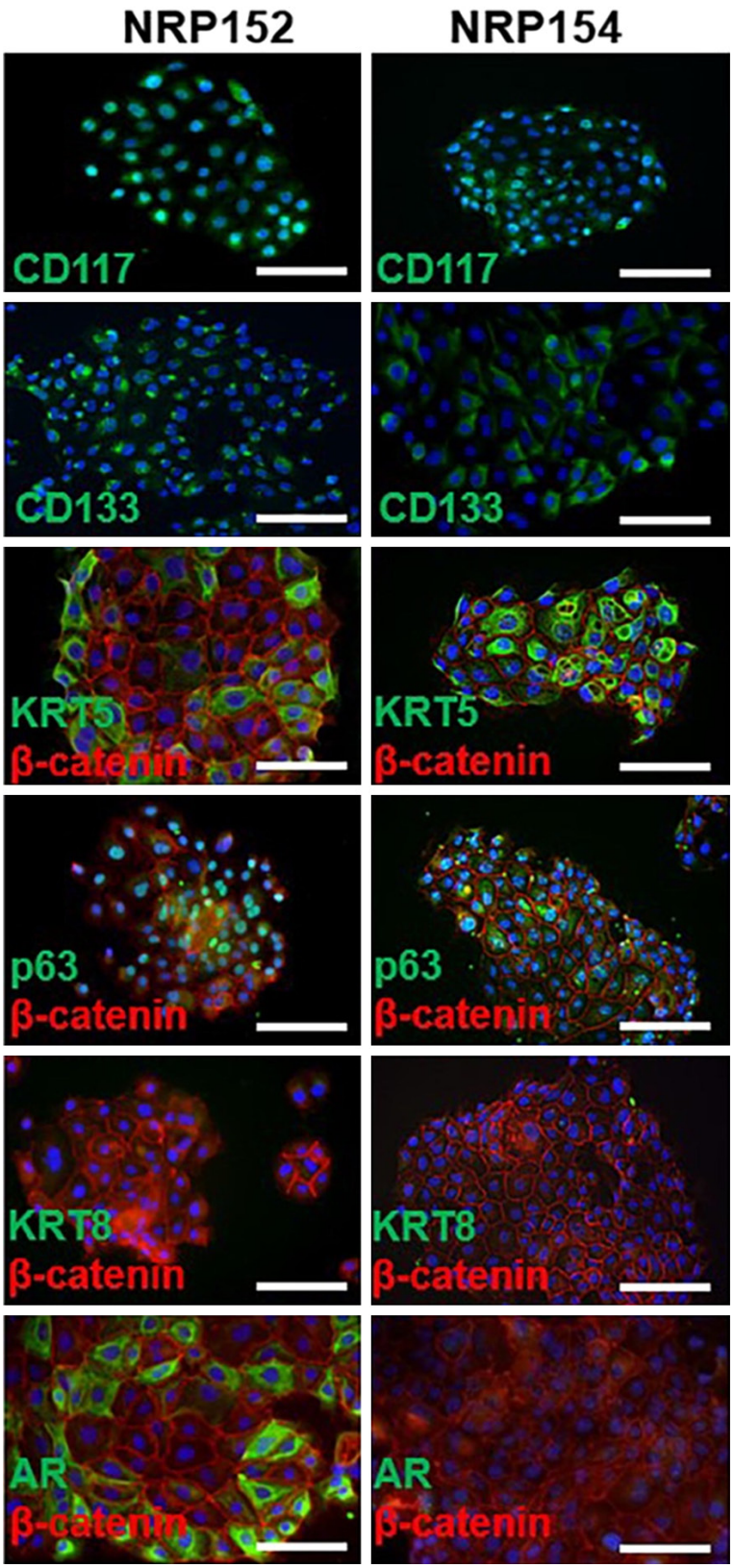

Figure 4. NRP152 and NRP154 prostasphere characterization using cell markers. Immunostaining of day 7 spheres derived from both NRP152 and NRP154 cells shows a subpopulation of stem cell markers CD117 and CD133 documenting stem cell presence at this time point. Both NRP152 and NRP154 cells are positive for prostate basal epithelial cell markers CK5 and p63 and negative for luminal epithelial cell marker CK8, indicating the basal cell phenotype of spheroids at this stage. A subpopulation of NRP152-derived spheroid cells is AR+ which was absent in NRP154-derived spheres. β-catenin (in red) is used as a counter stain to demarcate the cell membranes. Bar = 50 μm.

pamil treatment and is a readout of stem-like cells in 2D cultures. Using this approach, a very minor population of stem-like cells, 0.11 and 0.10% was found in the NRP152 and NRP154 cell cultures, respectively (**Figure 3A**). Next, prostaspheres were generated from NRP152 and NRP154 stem cells that form spheroids of proliferating and lineage-committing daughter progenitor cells in 3D Matrigel cultures (**Figure 3B**), as previously described [12-15]. Transfer of 500,000 NRP152/154 cells from 2D to 3D cultures yielded ~500 spheres on average for an efficiency of ~0.1%, supporting their origin from the minor stem cell population in the 2D cultures. The clonally derived spheres on day 7 continued to grow through a rapid proliferation of the daughter progenitor cells and enter lineage commitment by day 10 (**Figure 3B**).

Characterization of prostaspheres from NRP152 and NRP154 cells

To characterize the cell composition of day 7 prostaspheres from the two different NRP cell lines, ICC and IHC were undertaken using a variety of cell markers. As shown in **Figure 4**, a number of spheroid cells

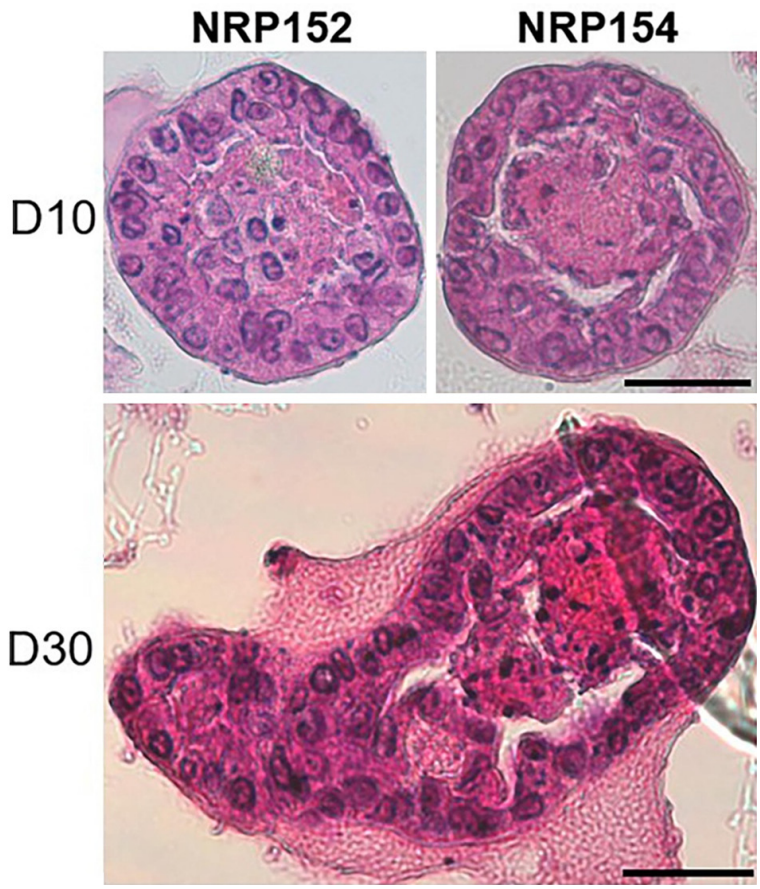

Figure 5. Differentiation ability of NRP152 and NRP154 cells. H&E staining of prostasphere cross-sections from NRP152 and NRP154-derived spheres reveals initial lumen formation at day 10. The continued growth of NRP154 spheres through day 30 shows tumoroid ductal formation. Epithelial cells in NRP154 spheres at days 10 and 30 show a cancerous phenotype with variable-sized and shaped nuclear morphology. Bar = 50 µm.

from both cell lines expressed CD117 and CD133, known surface markers for prostate stem cells [20, 21], indicating the continued presence of stem cells within the day 7 spheres. Daughter progenitor cells derived from the stem cell asymmetric cell division were identified as basal progenitor cells with positivity for CK5 and p63 in both NRP152- and NRP154-derived prostaspheres. In contrast, CK8 protein, a marker for luminal progenitors, was not detected in the day 7 spheres from either cell line. AR immunostaining was present in a subpopulation of the NRP152-generated spheres but not in spheres generated from NRP154 cells.

The prostaspheres from both cell lines were further grown for 10 and up to 30 days under spheroid culture conditions as shown in **Figure 5**. By day 10, lumen formation began to appear in both sphere types with cells in NRP154-derived spheres exhibiting a cancerous appearance based on abnormal nuclear morphology and prominent nucleoli at low magnification, phenotypes not seen in NRP152-derived spheres. Tumoroid ductal formation was apparent in NRP154 spheres grown to day 30, confirming their continued cancerous characteristics.

In vivo benign and cancerous prostate tissue reconstitution with renal grafts

We next sought to determine whether cancer stem-like and daughter progenitor cells from the tumorigenic NRP154 cell line were able to reseed tumor growth *in vivo*. Day 7 spheroids from both NRP152 and NRP154 cell lines were dispersed and 3000 cells per graft were mixed with rat embryonic UGM and grafted under the renal capsule of nude mice with continued growth for 1-4 months. Normal glandular prostate-like structures were formed from NRP152 stem/progenitor cells by 1 month with a continued normal phenotype with glandular secretions at 2 months (**Figure 6**). Immunostaining showed the bi-layered prostatic epithelium with basal cells ($p63^+$, $CK5^+$) and luminal epithelial cells ($CK8^+/18^+$) that expressed AR (**Figure 7**). Several cells were Ki-67+, typical for a growing structure.

In sharp contrast, NRP154-derived stem/progenitor cells produced large grafts exhibiting atypical hyperplasia and PIN by 1 month that progressed to poorly differentiated adenocarcinomas by 2-4 months (**Figures 6**, **8**). Immunostaining of grafts at 1 month revealed CK8/18+ luminal cells that were AR negative and lack of p63 stained basal cells. Ki-67^+ cells

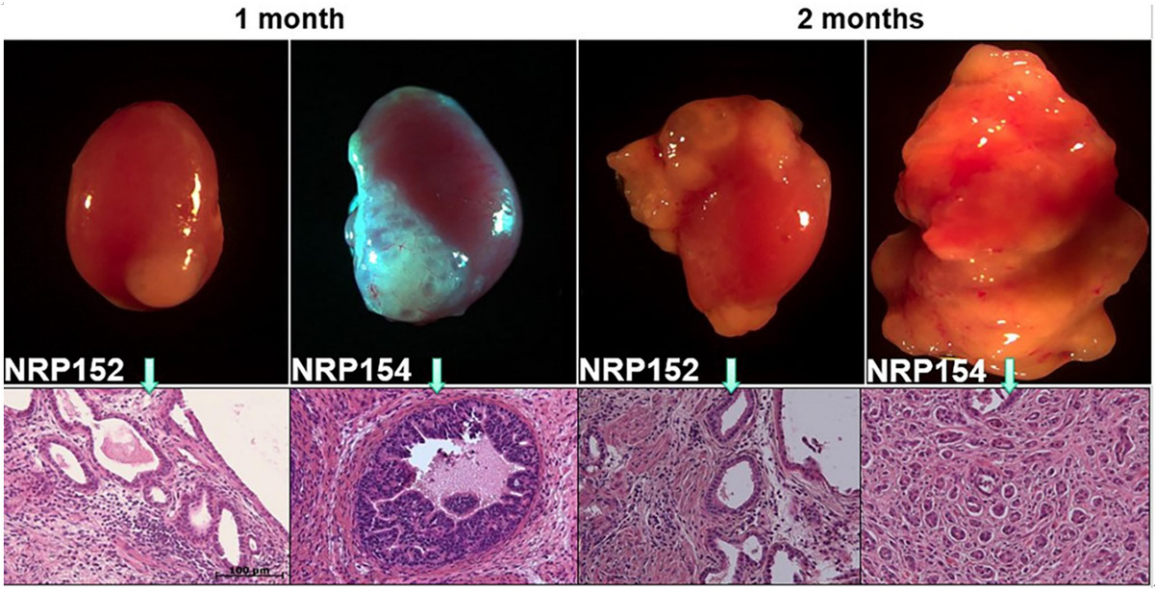

Figure 6. Renal grafts of NRP152 and NRP154 sphere-derived stem/progenitor cells recombined with rat UGM. NRP152-UGM recombinant cells formed normal prostate gland structures (top) and histology (bottom) at 1 month and 2 months. In contrast, renal grafts from NRP154 prostasphere cell recombinants developed epithelial hyperplasia, severe atypia, and high-grade PIN at 1 month, and grew to massive grafts that further progressed into poorly differentiated adenocarcinoma at 2 months. Bar = 100 μm.

were more numerous than observed in the NRP152 grafts, indicative of marked proliferative activity (**Figure 7**).

Several grafts were grown for 4 months to observe signs of further progression. The NRP152-derived grafts maintained their surface glandular structures separate from the kidney parenchyma with normal-appearing prostate-like tissue (**Figure 8**). In contrast, malignant progression to poorly differentiated tumors with invasion into the adjacent kidney parenchyma was observed in NRP154-derived tumors that in a few instances overtook the kidney structure (**Figure 8**). The poorly differentiated tumor cells remained p63- and CK8/18+.

Discussion

Overall, the present results document that tumorigenic NRP154 and nontumorigenic NRP-152 rat prostate epithelial cell lines contain a rare subpopulation of stem cells that are capable of reconstituting cancerous and benign tissues, respectively when combined with embryonic rat UGM and grafted under the kidney capsule in host nude mice. This provides clear evidence that prostate CSCs can repopulate new tumor growth outside the prostate gland that rapidly progresses to poorly differentiated adenocarcinoma with invasive capabilities. As such, this approach provides a novel model system for interrogating prostate CSC characteristics and propagation of tumor growth *in vivo*, an approach that likely can be applied to other PCa cell lines.

Accumulating evidence from cancer stem cell research suggests that a combination of conventional therapies that target bulk tumor cells and CSC-targeted therapies may be more effective in managing progressive cancer and cancer recurrence [25-32]. Research progress towards this goal for PCa has been limited by the availability of appropriate model systems for identifying and testing CSC therapeutic efficacy using combined *in vitro/in vivo* systems [33-35]. While some *in vitro* cancer stem cell assays and *in vivo* PCa animal models have been extensively used in the field [35], there is no PCa animal model directly derived from prostate CSCs. The dual *in vitro/in vivo* CSC model system presented herein provides this necessary platform for screening therapeutic agents that target prostate CSCs for effectively combined treatment protocols for local and advanced disease stages, including CRPC.

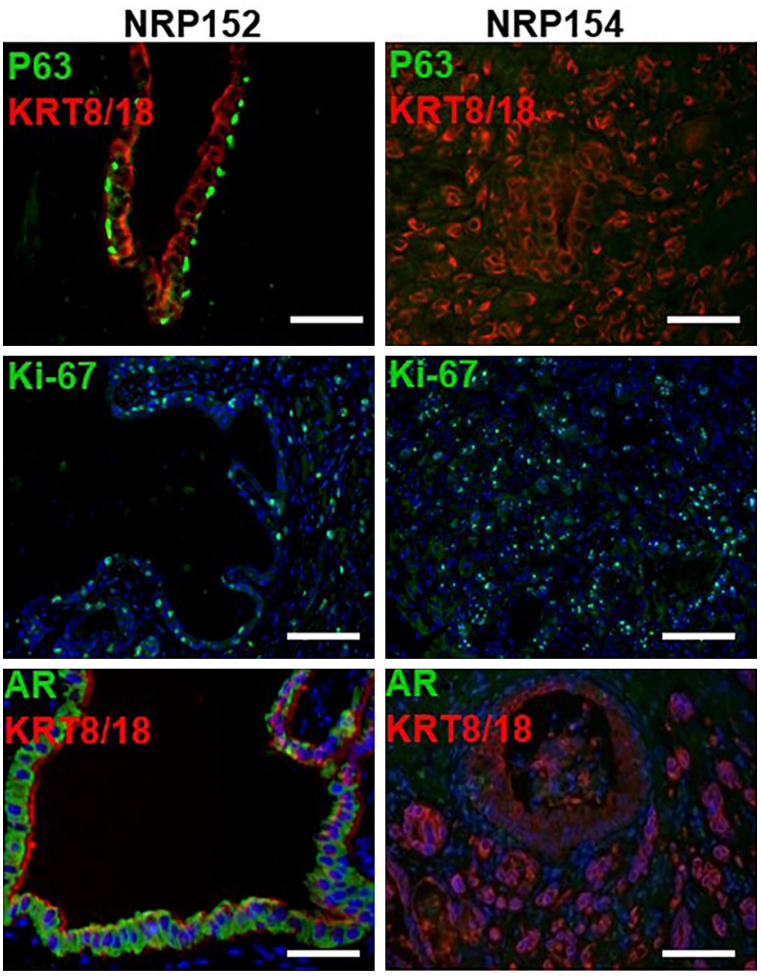

Figure 7. Characterization of renal grafts derived from NRP152 and NRP154 cells. Immunostaining of renal grafts shows normal basal (p63) and luminal (CK8/18) epithelial cell staining with AR+ in luminal cells of NRP152 prostasphere cell generated grafts. NRP154 stem/progenitor cell generated cancerous grafts are p63 negative, CK8/18 positive, and AR negative. The loss of basal cell markers in NRP154-derived grafts is a hallmark of cancer. Ki-67 staining showed moderate proliferation in the benign NRP152-derived grafts while there was exaggerated cancer epithelial cell proliferation in NRP154-generated tissue. Lack of AR in the cancer cells indicates an androgen-independent prostate cancer status. Bar = 50 μm.

Further, this tactic can be utilized with human PCa cell lines from different disease stages and carrying specific mutations, deletions, or transgenes for testing direct applicability to patients.

NRP152 and NRP154 cells are two congenic cell lines clonally derived from the dorsal-lateral prostate lobes of two carcinogen-treated Lobund/Wistar rats [7]. While both NRP152 and NRP154 cells were characterized as aneuploid, NRP152 cells are AR+, nontumorigenic, and considered premalignant while in contrast, NRP154 cells are AR- and tumorigenic. In the present studies, several oncogenic signaling molecules were examined to identify a molecular basis for the differential tumorigenic capabilities. While Pten, β-catenin, p-Akt, and e-cadherin levels were similar between the two lines, low levels of tumor suppressor gene caveolin-1 and increased activation of Src were observed in NRP154 cells as compared to NRP152 cells. Further, gene knockdown of caveolin-1 upregulated p-Src levels in NRP-152 cells resembling a pattern found in NRP154 cells. This suggests an important role of caveolin-1/p-Src signaling in driving the oncogenic activity of NRP154 cells [17-19]. By working with stem cells from premalignant NRP152 and malignant NRP154 cells in tandem, the model system presented herein has the potential for the discovery and testing of therapeutic targets that block CSC proliferation as well as preventing the full transformation of premalignant stem cells to CSCs that seed tumor growth.

The current study identified a small side population of stem-like cells in both NRP152 and NRP154 cell lines using the Hoechst exclusion assay which was confirmed by the formation of prostaspheres in 3D Matrigel cultures at an efficiency similar to stem-like cells observed by FACS. Immunostaining of prostate stem cell markers CD117 and CD133 further verified the stem/progenitor cell characteristics of prostasphere cells in day 7 cultures [20, 21]. Interestingly, different from the 2D cultures where NRP152 and NRP154 cells exhibit basal and luminal phenotypes respectively, prostasphere cells derived from both NRP152 and NRP154 stem cells stained positive with basal epithelial markers CK5 and p63, but negative for luminal

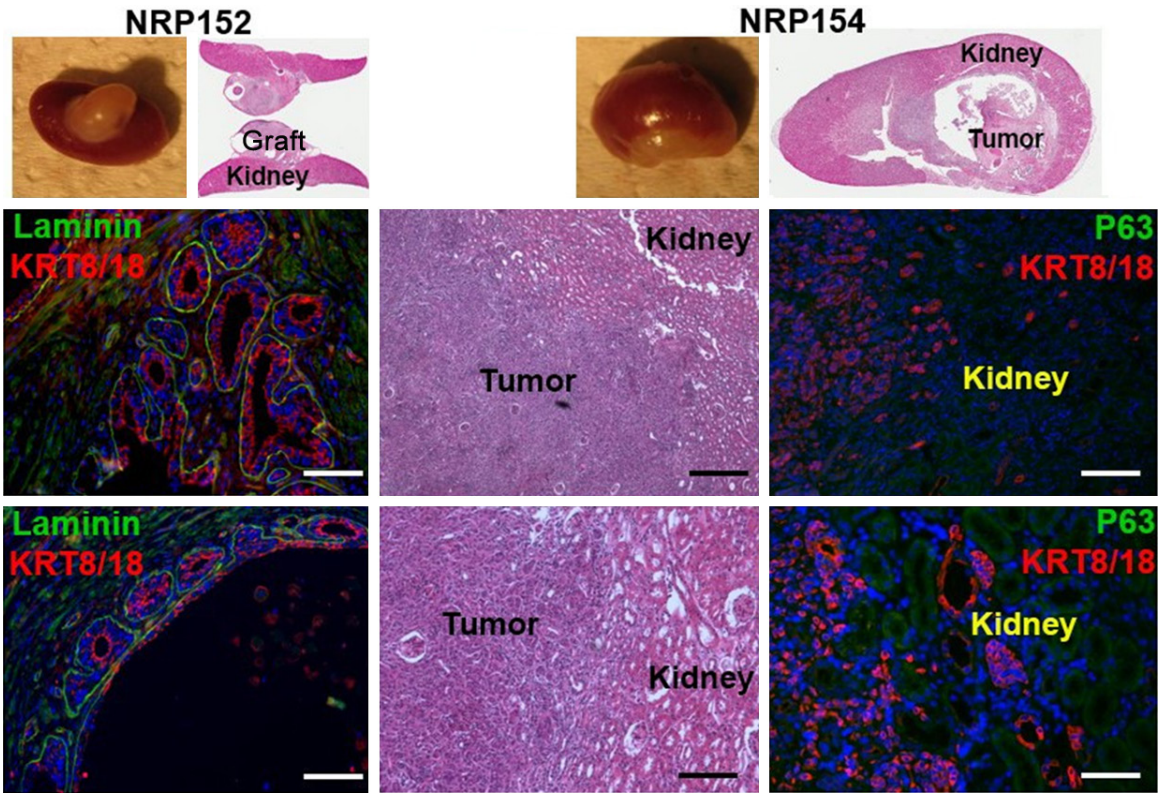

Figure 8. Kidney cross-section, H&E, and immunostaining of renal graft tissue at 4 months. NRP152 prostasphere cell-derived graft remained clearly separated from the kidney tissue where the graft was placed. The graft glandular structures showed CK8/18+ cells lining lumens and intact laminin-positive basement membranes (left panel). In sharp contrast, in NRP154 stem/progenitor cell-derived tumor grafts, the border between the tumor and kidney was missing as the cancer began invading into the kidney parenchyma. Kidney cross-sections and H&E staining show a tumor tissue invading and destroying the kidney structure. Immunostaining confirms CK8/18+/p63- NRP154 cancer cell invasion into the kidney tissue (right two panels). Bar = 50 μm.

marker CK8, supporting the plasticity of the stem cell populations from which the spheroids are derived, in particular the CSCs from NRP154. Nonetheless, only NRP152 spheroids produced progeny that were AR+ while NRP154 derived spheres remained AR- through extended *in vitro* growth for 30 days and *in vivo* growth as renal grafts suggesting a permanent silencing of the AR gene as indicated by Northern blots in the parental cell line [7]. In the original studies by the Danielpour lab, the tumorigenic ability of NRP154 cells was documented using subcutaneous grafts where 3×10^6 cells were required to establish a palpable tumor [7]. Using 1×10^5 NRP152 cells from 2D cultures mixed with UGM, the Cunha lab generated prostate structures in a renal graft system [8]. In the present studies using enriched stem/progenitor cells from NRP152 or NRP154-derived prostaspheres, only 3,000 cells combined with UGM were required for robust growth as renal grafts, forming normal prostate glandular structures and tumor tissue respectively, documenting the high regenerative ability of the spheroid-derived stem/progenitor cells. The continued growth of tumor grafts from NRP154 cells for 2-4 months enabled oncogenic progression leading to the local invasion of cancer cells into kidney tissue, suggesting the establishment of a high-aggressiveness tumor model derived from NRP154 CSCs.

In summary, the present studies have established a PCa model system that mimics CSC-propagated tumor growth and invasion. This unique CSC-derived model will provide the necessary experimental tools to study prostate CSC biomarkers and to screen drugs for potential CSC-targeted therapies.

Acknowledgements

This research was supported in part by NIH grants RC2-ES018758 and R01-CA166588.

We acknowledge Dr. David Danielpour from Case Western University for generously sharing NRP152 and 154 cell lines.

Disclosure of conflict of interest

None.

Address correspondence to: Drs. Wen-Yang Hu and Gail S Prins, Department of Urology, University of Illinois at Chicago, 840 S. Wood Street, Ste 132, M/C 955, Chicago, IL60612-4325, USA. E-mail: wyhu@uic.edu (WYH); gprins@uic.edu (GSP)

References

[1] American Cancer Society. Facts & Figures 2022. American Cancer Society. Atlanta, Ga; 2022.

[2] Harris KS and Kerr BA. Prostate cancer stem cell markers drive progression, therapeutic resistance, and bone metastasis. Stem Cells Int 2017; 2017: 8629234.

[3] Chen X, Li Q, Liu X, Liu C, Liu R, Rycaj K, Zhang D, Liu B, Jeter C, Calhoun-Davis T, Lin K, Lu Y, Chao HP, Shen J and Tang DG. Defining a population of stemlike human prostate cancer cells that can generate and propagate castration resistant prostate cancer. Clin Cancer Res 2016; 22: 4505-16.

[4] Portillo-Lara R and Alvarez MM. Enrichment of the cancer stem phenotype in sphere cultures of prostate cancer cell lines occurs through activation of developmental pathways mediated by the transcriptional regulator ΔNp63α. PLoS One 2015; 10: e0130118.

[5] Sánchez BG, Bort A, Vara-Ciruelos D and Díaz-Laviada I. Androgen deprivation induces reprogramming of prostate cancer cells to stem-like cells. Cells 2020; 9: 1441.

[6] Leão R, Domingos C, Figueiredo A, Hamilton R, Tabori U and Castelo-Branco P. Cancer stem cells in prostate cancer: implications for targeted therapy. Urol Int 2017; 99: 125-136.

[7] Danielpour D, Kadomatsu K, Anzano MA, Smith JM and Sporn MB. Development and characterization of nontumorigenic and tumorigenic epithelial cell lines from rat dorsal-lateral prostate. Cancer Res 1994; 54: 3413-21.

[8] Hayward SW, Haughney PC, Lopes ES, Danielpour D and Cunha GR. The rat prostatic epithelial cell line NRP-152 can differentiate in vivo in response to its stromal environment. Prostate 1999; 39: 205-212.

[9] Danielpour D. Transdifferentiation of NRP-152 rat prostatic basal epithelial cells toward a luminal phenotype: regulation by glucocorticoid, insulin-like growth factor-I and transforming growth factor-beta. J Cell Sci 1999; 112: 169-79.

[10] Huang L, Pu Y, Hepps D, Danielpour D and Prins GS. Posterior Hox gene expression and differential androgen regulation in the developing and adult rat prostate lobes. Endocrinology 2007; 148: 1235-45.

[11] Chen Z, Bakhshi FR, Shajahan AN, Sharma T, Mao M, Trane A, Bernatchez P, van Nieuw Amerongen GP, Bonini MG, Skidgel RA, Malik AB and Minshall RD. Nitric oxide-dependent Src activation and resultant caveolin-1 phosphorylation promote eNOS/caveolin-1 binding and eNOS inhibition. Mol Biol Cell 2012; 23: 1388-98.

[12] Hu WY, Shi GB, Hu DP, Nelles JL and Prins GS. Actions of endocrine disrupting chemicals on human prostate stem/progenitor cells and prostate cancer risk. Mol Cell Endocrinol 2012; 354: 63-73.

[13] Hu WY, Shi GB, Lam HM, Hu DP, Ho SM, Madueke IC, Kajdacsy-Balla A and Prins GS. Estrogen-initiated transformation of prostate epithelium derived from normal human prostate stem-progenitor cells. Endocrinology 2011; 152: 2150-2163.

[14] Prins GS, Hu WY, Shi GB, Hu DP, Majumdar S, Li G, Huang K, Nelles JL, Ho SM, Walker CL, Kajdacsy-Balla A and van Breemen RB. Bisphenol A promotes human prostate stem-progenitor cell self-renewal and increases in vivo carcinogenesis in human prostate epithelium. Endocrinology 2014; 155: 80517.

[15] Xin L, Lukacs RU, Lawson DA, Cheng D and Witte ON. Self-renewal and multilineage differentiation in vitro from murine prostate stem cells. Stem Cells 2007; 25: 2760-9.

[16] Prins GS, Birch L and Greene GL. Androgen receptor localization in different cell types of the adult rat prostate. Endocrinology 1991; 129: 3187-99.

[17] Díaz MI, Díaz P, Bennett JC, Urra H, Ortiz R, Orellana PC, Hetz C and Quest AFG. Caveolin-1 suppresses tumor formation through the inhibition of the unfolded protein response. Cell Death Dis 2020; 11: 648.

[18] Varkaris A, Katsiampoura AD, Araujo JC, Gallick GE and Corn PG. Src signaling pathways in prostate cancer. Cancer Metastasis Rev 2014; 33: 595-606.

[19] Dehm SM and Bonham K. SRC gene expression in human cancer: the role of transcriptional activation. Biochem Cell Biol 2004; 82: 263-74.

[20] Leong KG, Wang BE, Johnson L and Gao WQ. Generation of a prostate from a single cell. Nature 2008; 456: 804-8.

[21] Vander Griend DJ, Karthaus WL, Dalrymple S, Meeker A, DeMarzo AM and Isaacs JT. The role

of CD133 in normal human prostate stem cells and malignant cancer-initiating cells. Cancer Res 2008; 68: 9703-11.
[22] Housman G, Byler S, Heerboth S, Lapinska K, Longacre M, Snyder N and Sarkar S. Drug resistance in cancer: an overview. Cancers (Basel) 2014; 6: 1769-92.
[23] Esmatabadi MJ, Bakhshinejad B, Motlagh FM, Babashah S and Sadeghizadeh M. Therapeutic resistance and cancer recurrence mechanisms: unfolding the story of tumour coming back. J Biosci 2016; 41: 497-506.
[24] Rezayatmand H, Razmkhah M and Razeghian-Jahromi I. Drug resistance in cancer therapy: the Pandora's Box of cancer stem cells. Stem Cell Res Ther 2022; 13: 181.
[25] Flemming A. Targeting the root of cancer relapse. Nat Rev Drug Discov 2015; 14: 165.
[26] Marzagalli M, Fontana F, Raimondi M and Limonta P. Cancer stem cells-key players in tumor relapse. Cancers (Basel) 2021; 13: 376.
[27] Masciale V, Banchelli F, Grisendi G, D'Amico R, Maiorana A, Stefani A, Morandi U, Stella F, Dominici M and Aramini B. The influence of cancer stem cells on the risk of relapse in adenocarcinoma and squamous cell carcinoma of the lung: a prospective cohort study. Stem Cells Transl Med 2022; 11: 239-247.
[28] Phi LTH, Sari IN, Yang YG, Lee SH, Jun N, Kim KS, Lee YK and Kwon HY. Cancer stem cells (CSCs) in drug resistance and their therapeutic implications in cancer treatment. Stem Cells Int 2018; 2018: 5416923.
[29] Wolf I, Gratzke C and Wolf P. Prostate cancer stem cells: clinical aspects and targeted therapies. Front Oncol 2022; 12: 935715.
[30] Mei W, Lin X, Kapoor A, Gu Y, Zhao K and Tang D. The contributions of prostate cancer stem cells in prostate cancer initiation and metastasis. Cancers (Basel) 2019; 11: 434.
[31] Li JJ and Shen MM. Prostate stem cells and cancer stem cells. Cold Spring Harb Perspect Med 2019; 9: a030395.
[32] Skvortsov S, Skvortsova II, Tang DG and Dubrovska A. Concise review: prostate cancer stem cells: current understanding. Stem Cells 2018; 36: 1457-1474.
[33] Cheng L, Ramesh AV, Flesken-Nikitin A, Choi J and Nikitin AY. Mouse models for cancer stem cell research. Toxicol Pathol 2010; 38: 62-71.
[34] Aiken C and Werbowetski-Ogilvie T. Animal models of cancer stem cells: what are they really telling us? Curr Pathobiol Rep 2013; 1: 91-99.
[35] Valkenburg KC and Williams BO. Mouse models of prostate cancer. Prostate Cancer 2011; 2011: 895238.